ISAAC TESTS

Gert Finger

1.0 Test 1 17.12 96 - 23.12.96

1.1 Dark current measurement

The dark current was measured at a voltage of 1.020 V across the on chip Si diode temperature sensor corresponding to 55 K (65 K SBRC data sheet). The signal versus time is plotted in figure 1.

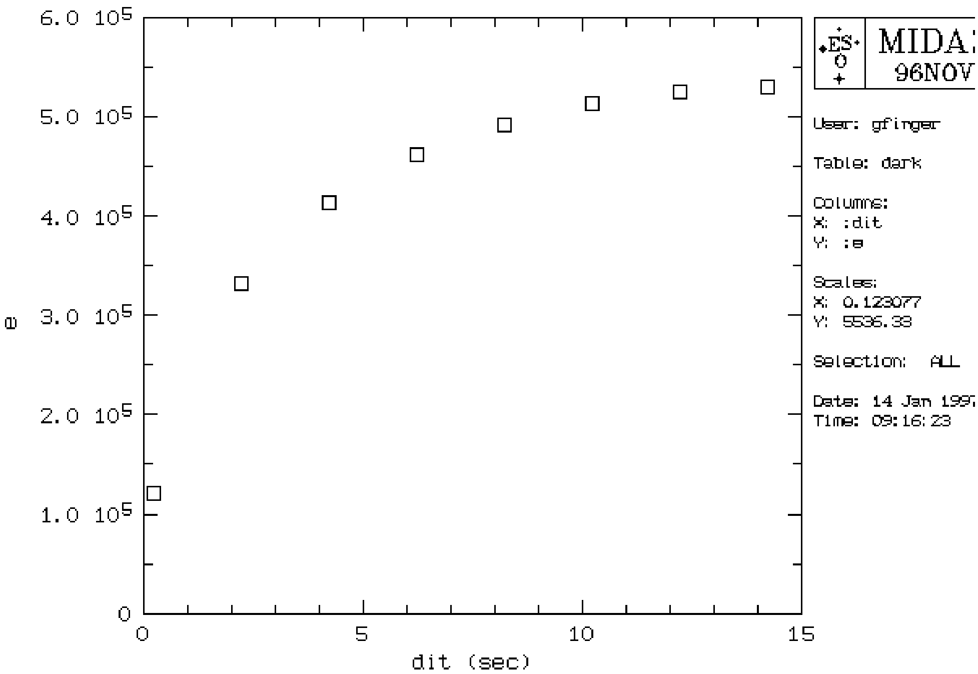

FIGURE 1. Dark frames versus time

Based on previous PTF measurements 1 ADU corresponds to 20 e.The dark current is 10^5 e/sec. The nonlinear discharge curve indicates that the darks are completely detector dark current limited. The detector temperature is too high. Previous dark current measurements are consistent with this measurement if the detector temperature is 55 K. The detector temperature of the conductus temperature controller was 35 K. A temperature difference of 20 K is measured between the detector temperature sensor and the on-chip temperature sensor.For comparison, in IRATEC the dark current was 200 e/sec at 30 K. The temperature difference between detector and cold finger sensor was 5 K.

1.2 Focus of star simulator wrt slit

The fiber of the star simulator was scanned across the slit by changing the focus in steps of 5 mm. The integrated flux is plotted versus fiber position in figure 2. Each curve corresponds to a different focus position. The slope of the curves does not change with focus position which cannot be explained.

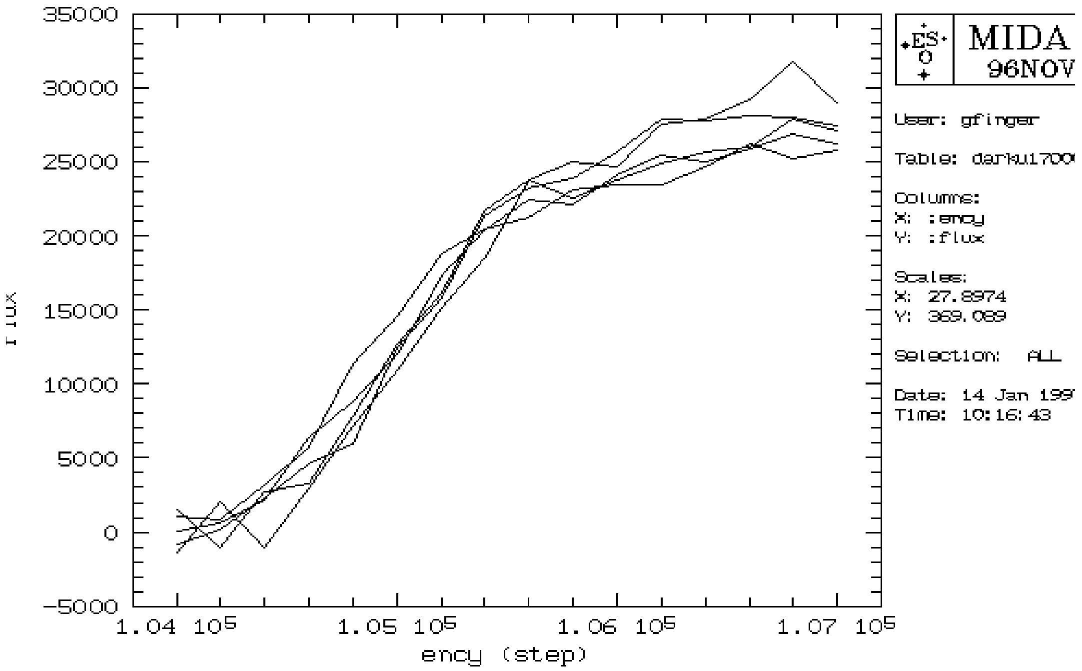

FIGURE 2. Point source scanned across slit.Each curve corresponds to different focal position which was changed from 85 mm to 105 mm in steps of 5 mm.

When the point source starts to enter the slit it is elongated perpendicular to the slit (figure 3). In the slit it is circular (figure 4).

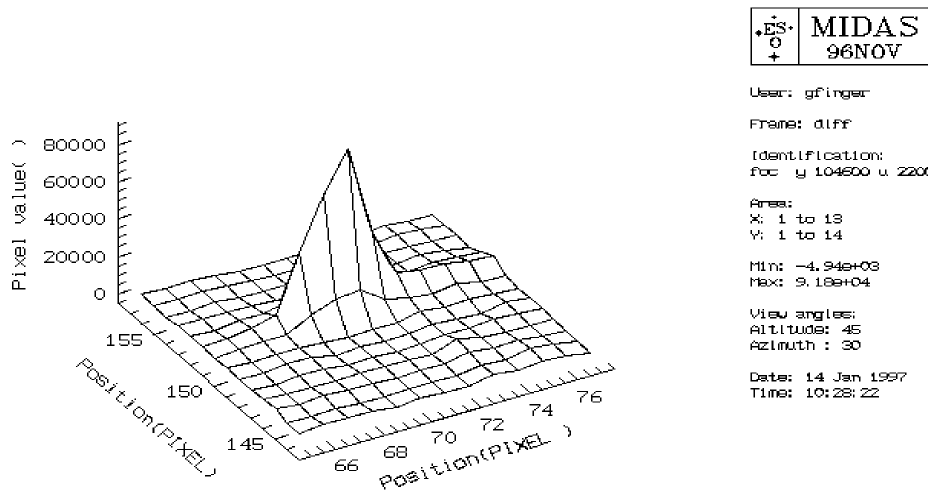

FIGURE 3. Spot is partly cut by slit

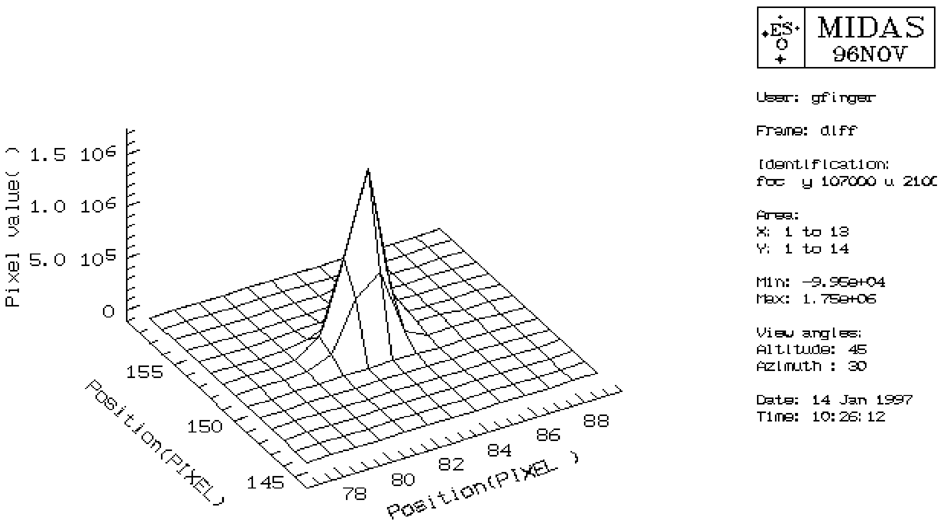

FIGURE 4. Point is completely inside slit

1.3 Efficiency in K' band

The saturation curve was measured in K as seen in Figure . The signal current is 4.82 10^5 e/sec. The photon flux expected with L2 ($f^{\#}$=4.718) in K' is 3.7 10^4 photons/sec at T=20 Celsius. With the dark current value of 10^5 e/sec the measured photo current would be 3.8 10^5 photons/sec which is a factor of 10 too high. It may be possible, that the detector temperature has changed between K' and dark current measurements.

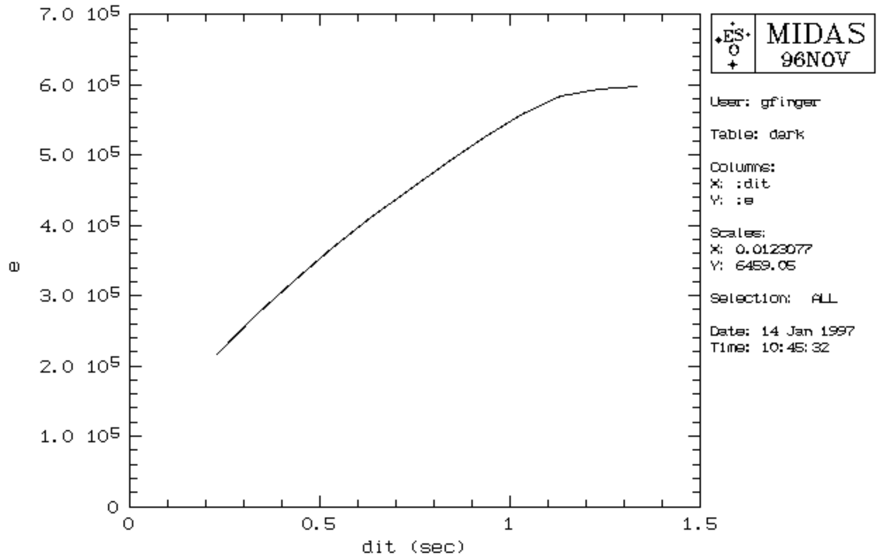

FIGURE 5. Signal versus integration time in K

1.4 Conclusions

One of the main problem is the cryogenics. The detector is too warm. The heat sinking of the detector is insufficient. The dark current is 10^5 e/sec at 55 K. The measured flux in K' is too high by one order of magnitude.

The scan of the point source across the slit did not yield the focus of the star simulator wrt to the slit which is not understood.

1.5 Remark

A reduction of the distance detector - L2 by 2.3 mm corresponds to 23 mm at the telescope focus or 98000 encoder steps. From figure 1 of J. Cuby this seems to overcompensate the misalignment.

2.0 Test 2

The rms noise is 4 ADU at RT with cables free. 5 ADU with detector cover. 12 ADU with bias and clock cable thermalized using varnish. The detector braid was touching components on the detector board. Detector moved 1.8 mm.

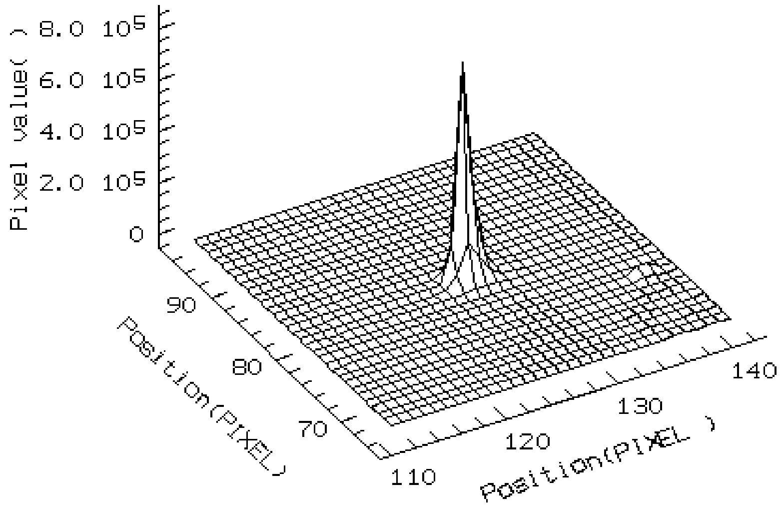

FIGURE 6. Image of star simulator in narrow band K (λ=2.28 µm). FWHM = 1.25 pixels. 36% of energy in one pixel. Star simulator is 28 mm from zero position.The image was obtained by centering the intensity on one pixel.(raw724-raw725)

2.1 Comparison of image position spectroscopy imaging

The images were created by a 100 mm pinhole in the mask of the slitmaskwheel. The blackbody illuminating the pinhole through the star simulator was set to 300 C using a shutter both in the on and off position. Filter was K narrow band (λ=2.28 µm).

In spectroscopy mode the grating was set to zero order. Image position is (x=133.31pixels, y=77.91 pixels). Grating is at 653481 encoders. (raw 801).The image has a FWHM of 4 pixels. Shifting the grating by 200 encoder steps moves the image to (x=86.2pixels, y=76.6 pixels).

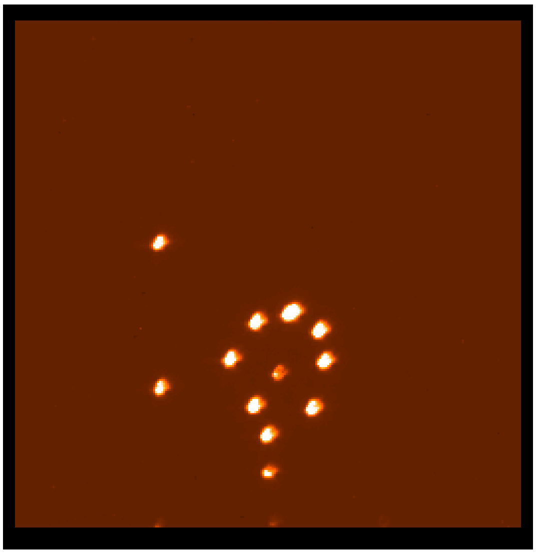

FIGURE 7. Zero order image of mask pinhole

If the grating drive position is switched from the zero order position to the mirror position the image position is (x=117.55pixels, y=83.60 pixels). Grating is at 233400 encoders. (raw1298).The image has a FWHM of 4 pixels.

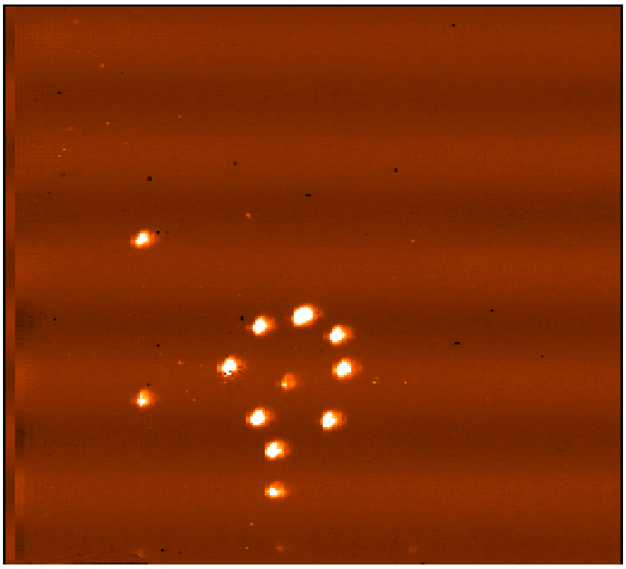

FIGURE 8. Image of mask pinhole with grating in the mirror position.

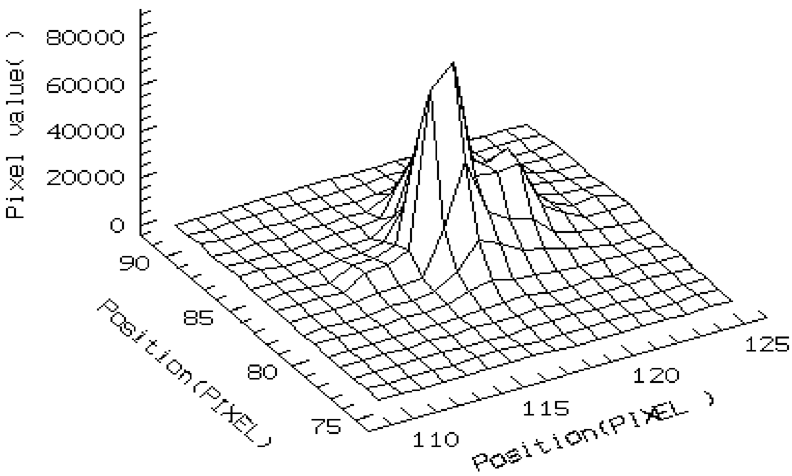

FIGURE 9. Image of mask pinhole with grating in the mirror position.FWHM 4 pixels

In imaging mode the blackbody temperature had to be reduced to 195 C in order to avoid saturation. Image position is (x=135.73 pixels, y=141.73 pixels). (raw 794).The image has a FWHM of 4.2 pixels.

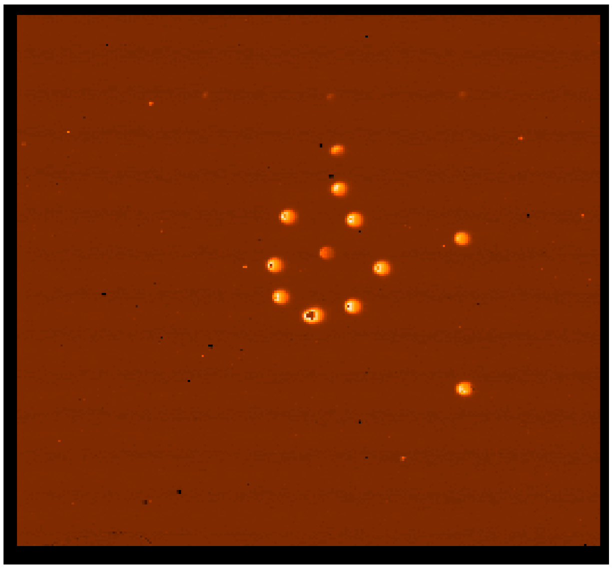

FIGURE 10. Image of mask pinhole in imaging mode

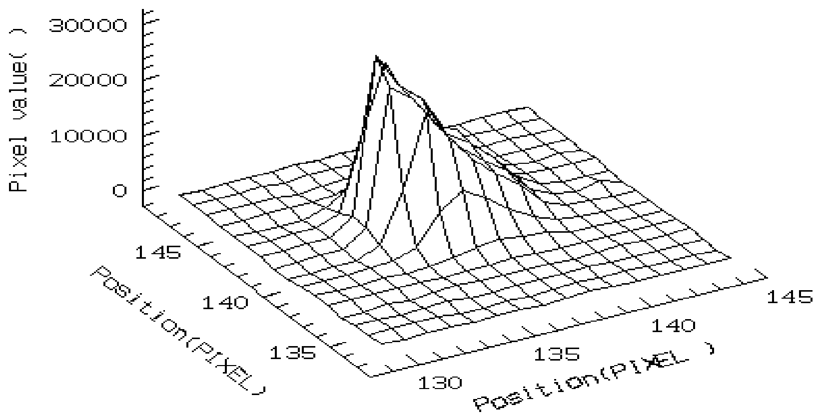

FIGURE 11. Image of mask pinhole in imaging mode. FWHM 4 pixels

TABLE 1. Position of mask pinhole

mode	x,y position [pixels]
imaging	135.73, 141.73
spectroscopy mirror	117.55, 83.60
spectroscopy zero order	133.31, 77.91

2.2 Dark measurement

With the mask wheel filter wheel and lens wheel all in dark position the dark current is ~ 1200 e/sec depending on the position in the field.

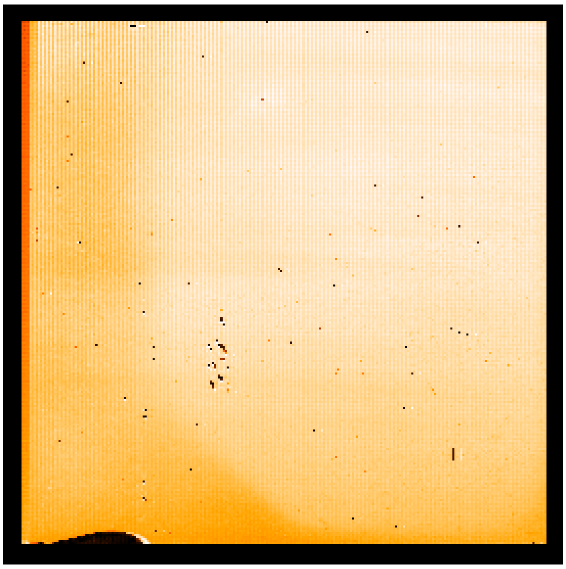

FIGURE 12. Dark exposure. Integration time 260 sec. cuts=0,2E5. Sum of 10 exposures.

Since the dependence of signal versus time is linear the dark current is dominated by the photo current which is independent of the voltage across the detector diode. The QE of the detector is ~ 1. Hence, 1 electron corresponds to 1 photon. The images are the sum of 10 exposures. 1 ADU is assumed to correspond to 20 e. The saturation level is at 190000 ADU corresponding to 380000 e. The measured dark current represents the thermal background photon flux in ISSAC and varies across the field between 1200 photons/sec and 1500 photons/sec.

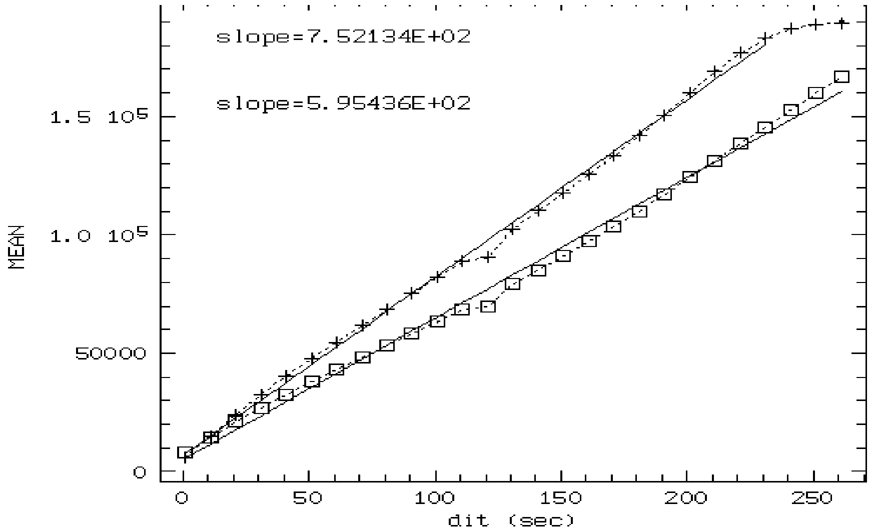

FIGURE 13. Thermal background flux in ISAAC. 1 ADU corresponds to 20 photons. Linear dependence on integration time indicates that photo current is dominating detector dark current.

To understand the origin of the thermal background the photon flux was measured with a dark in the lens wheel and a dark in the filter wheel. The result is confusing.

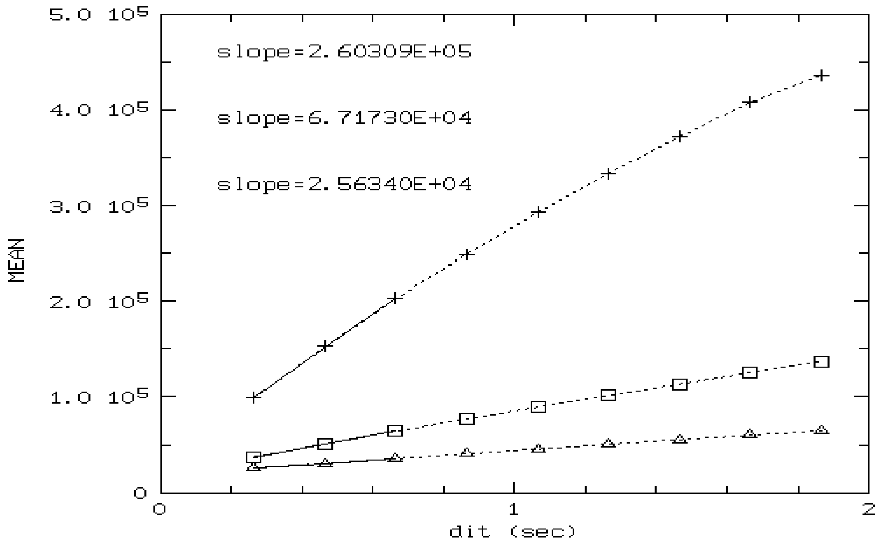

FIGURE 14. Comparison of photon flux: dark position in filter wheel: 2.6E5 phot/sec, dark position in lens wheel 6.7E4 photons/sec, K’ without dark 2.5E4 photons/sec

Remark: Due to a software problem all filters are shifted by one position and the filter positions given in Figure 14 are not correct.

2.3 Efficiency

2.3.1 Efficiency measured with ambient temperature radiation

Looking into ambient background at 20 C the a series of exposures was taken increasing the integration time from 1 second to 10 seconds in steps of 1 second. The average signal versus integration time is shown in Figure 15. The slope of the saturation curve is 1865 ADU's/sec. Since the signal is the sum of 2 measurements and 1 ADU is assumed to correspond to 20 electrons, the signal current is 1865 e/sec

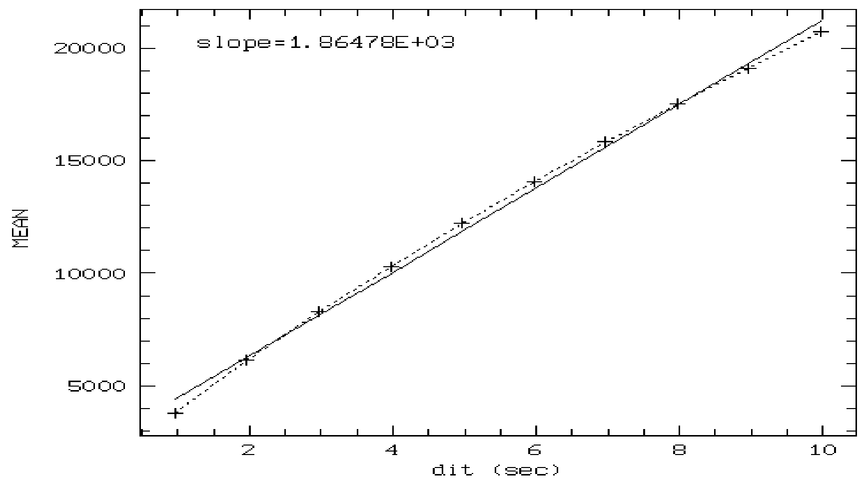

FIGURE 15. Signal versus detector integration time looking into ambient background using K' filter in imaging mode. Signal is sum of 2 integrations. Instrument efficiency is 84%

The photon flux arriving at the detector can be calculated by multiplying the photon flux of the Planck radiation for objective L2 having a focal ratio of f / 4.718 with the measured filter transmission of filter K' as shown in Figure 16. The integrated flux is $3.577\ 10^4$ photons/sec.

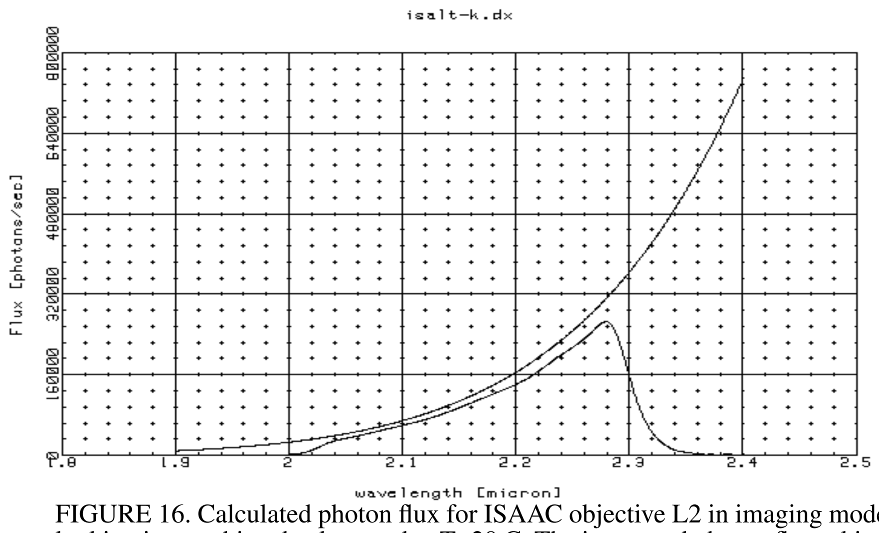

FIGURE 16. Calculated photon flux for ISAAC objective L2 in imaging mode looking into ambient background at T=20 C. The integrated photon flux taking into account the filter transmission only is $3.577\ 10^4$ photons/sec.

The quantum efficiency of the detector is 62% at 50 K. The resulting overall efficiency excluding the filter transmission but including the detector QE is 52%. The instrument efficiency excluding the detector QE is 84%. The predicted efficiency including the entrance window ($\tau = 0.94$), the mode selector mirror ($\tau = 0.99$), the BaF_2 collimator lens ($\tau = 0.92$) and the objective L2 ($\tau = 0.95$) and the detector (QE = 0.62) is η_{TOTAL}= 0.53 which is close to the observed value.

efficiency in L 0.31

2.3.2 Efficiency measured with blackbody

A blackbody was heated to 70 C and re-imaged to the telescope focal plane by the star simulator. A shutter in front of the blackbody was opened and closed and the difference of the images was used to derive the efficiency. The number of photons arriving at the detector was calculated by dividing the Planck curve by the photon energy and multiplying it by the filter transmission measured at cryogenic temperatures. The solid angle was calculated using the focal ratio f#=4.7182 of objective L2. The integrated photon flux for the shutter in the open position is 9.104E5 photons/sec as shown in Figure 17. For the shutter in the closed position the flux of the blackbody at a temperature of 20 C is 3.577E4 photons/sec yielding a net photon flux for the difference of 8.746E5 photons/sec.

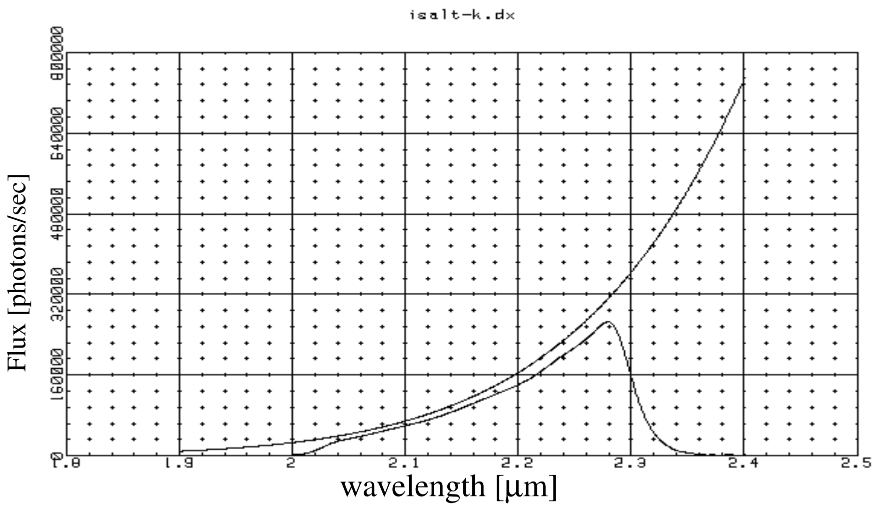

FIGURE 17. Calculated photon flux for ISAAC objective L2 in imaging mode looking into blackbody at T=70 C.

The measured flux was derived by varying the integration time from 100 msec to 600 msec in steps of 100 msec and calculation the slope of the integration ramp as shown in Figure 18. The slope is 1.797E6 ADU's/sec. Using a PTF of 20 e/ADU the photocurrent is 3.594E5 e/sec and the overall efficiency of the instrument excluding the filter transmission is 41%.

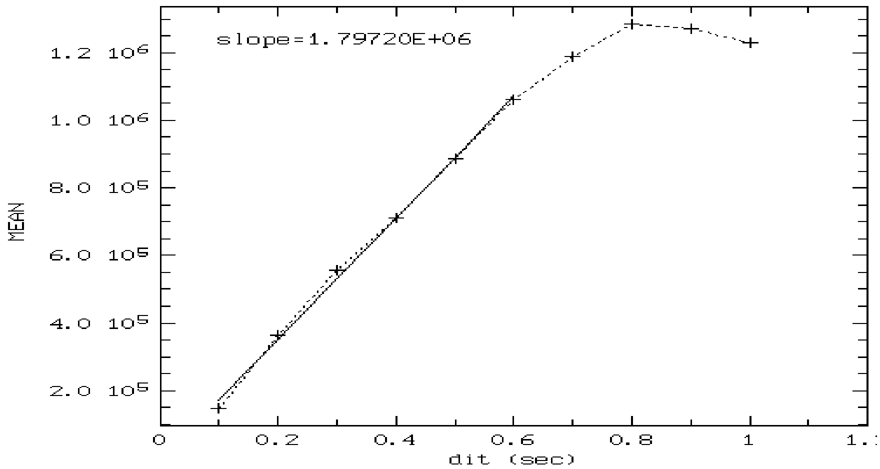

FIGURE 18. Signal of the sum of 100 exposures versus integration time looking into a blackbody of T= 70 C. Slope = 1.797E4 ADU's/sec for a single exposure.

The expected efficiency is the product of the efficiency of all optical elements, namely the lenses of the star simulator (τ = 0.883), the entrance window (τ = 0.94), gold mirrors M1 and M7 (τ = 0.98), the collimator lens (τ = 0.92), the objective L2 (τ = 0.95) and the quantum efficiency of the detector (QE = 0.62) yielding the overall expected efficiency of 44%. This value is in reasonable agreement with the measured efficiency of 41%.

2.3.3 Efficiency of the spectroscopic arm

The efficiency of the spectroscopic arm was measured in the narrow band filter at λ=2.28 µm. A Ne lamp was imaged onto the slit by the star simulator. The integrated intensity of the slit between row 64 and row 192 is 71431 ADU's in the imaging mode. The sum of the integrated intensities of 6 Ne lines is listed in Table 2 for the spectroscopic mode. The lines at λ < 2.25304 µm have not been included. Therefore the predicted efficiency is slightly pessimistic. The efficiency of the spectroscopic is arm including the grating, the three mirror collimator and M2 (7 reflections and grating) is 23%. This value is low and may be due to a serious misalignment of the pupil image.

TABLE 2. Efficiency of spectroscopic arm and integrated line intensities in narrow band K filter at λ=2.28 µm

number	wavelength [µm]	Integrated line intensity [ADU]	Total intensity [ADU]
1	2.25304	6923	Spectroscopy:
2	2.26618	6105	16378
3	2.26878	1349	Imaging:
4	2.31005	1498	71431
5	2.32603	213	Efficiency:
6	2.33730	289	23%

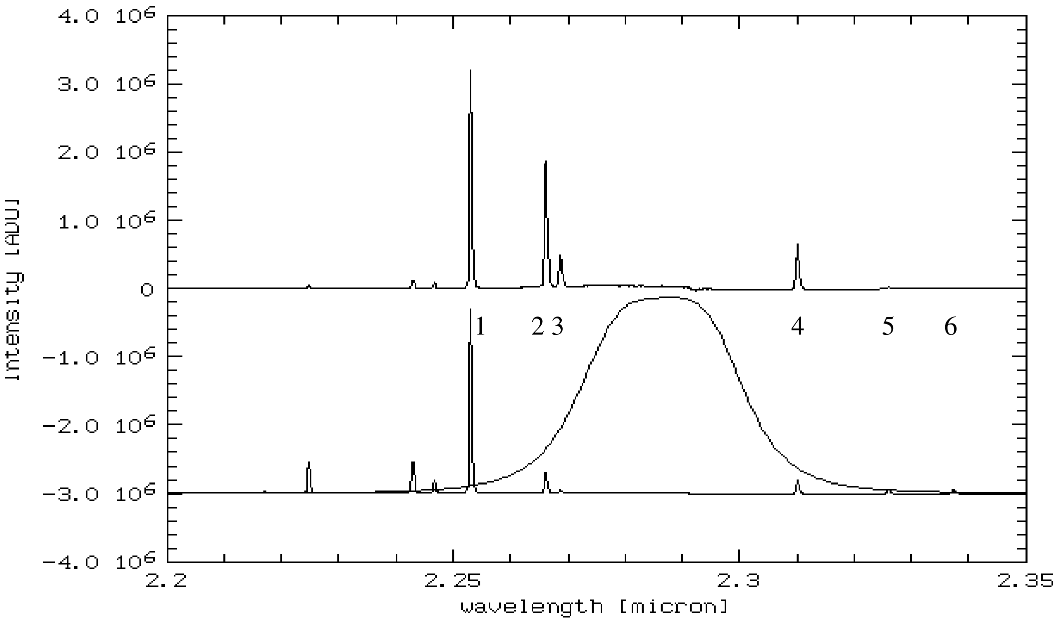

FIGURE 19. Upper curve: Ne spectrum multiplied with transmission of narrow band filter at λ=2.28 µm. Middle curve: transmission of narrow band filter. Lower curve: Ne spectrum measured with broad band filter K', offset for clarity and scaled for this plot (only relative intensities can be compared). Line numbers as indicated in Table 2 .

The relative line intensities indicate that the transmission peak of the narrow band filter is at slightly longer wavelengths than measured with the FTS.

2.4 Extrafocal image quality

The nominal focus of the star simulator is at 33 mm. (u encoder position 330000, 10000 encoder steps /mm, attention in x,y 2000 encoder steps/mm). To assess the image quality, a grid of 6x6 positions of extrafocal images at 28 mm has been taken and some of these images are shown in Figure 20 to Figure 28. The extrafocal position used for theses images is 5 mm closer to the entrance window than the nominal focus position.All images are elongated in the horizontal direction (coma?). The square shown in the figures indicates the position of the magnified subimages relative to the FOV of the complete array. The subimages contain 16x16 pixels.

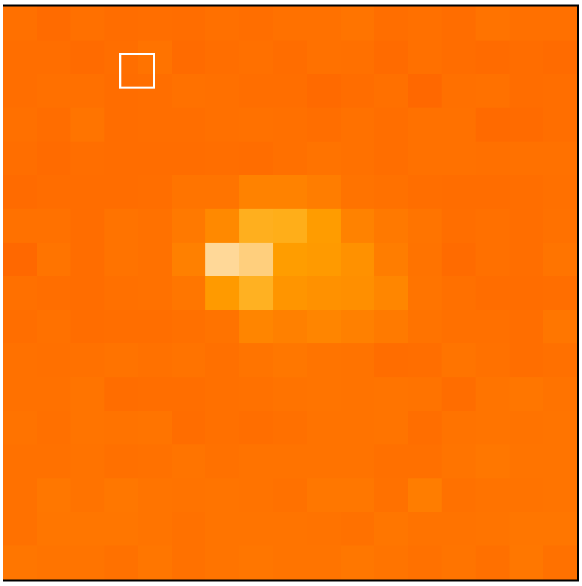

FIGURE 20. Out of focus point image at focus 28 mm (x = 56 to 72 pixels, y = 234 to 250 pixels). Nominal focus 33 mm.

.

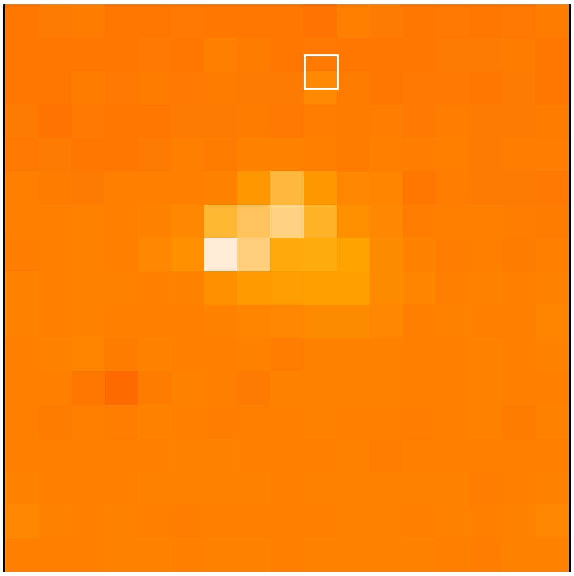

FIGURE 21. Out of focus point image at focus 28 mm (x = 145 to 161 pixels, y= 232 to 248 pixels). Nominal focus 33 mm.

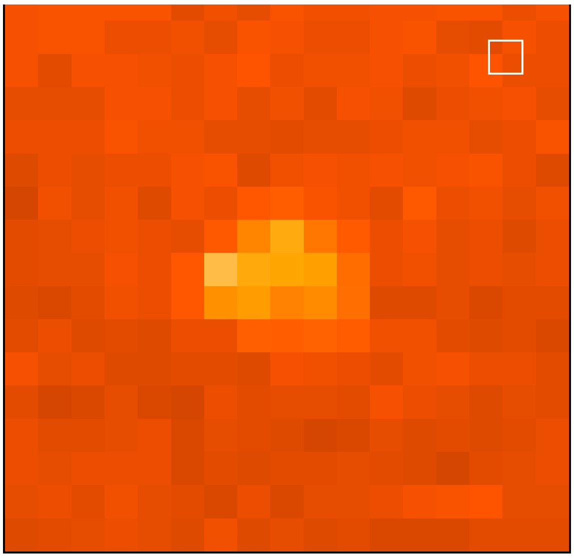

FIGURE 22. Out of focus point image at focus 28 mm (x = 234 to 250 pixels, y= 231 to 247 pixels). Nominal focus 33 mm.

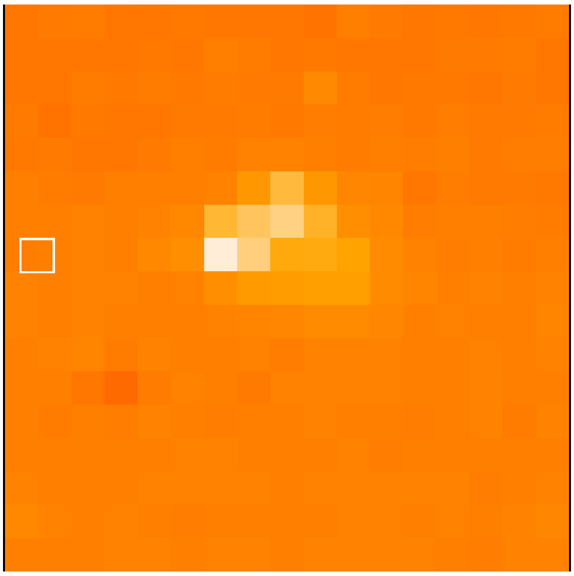

FIGURE 23. Out of focus point image at focus 28 mm (x = 8 to 24 pixels, y= 144 to 160 pixels). Nominal focus 33 mm.

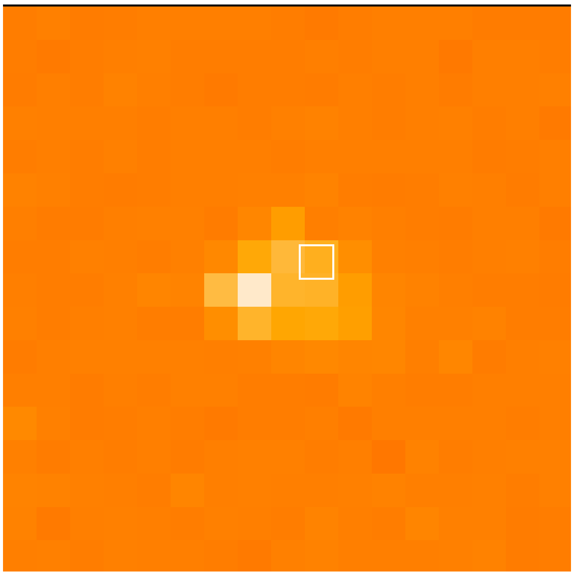

FIGURE 24. Out of focus point image at focus 28 mm (x = 138 to 154 pixels, y= 144 to 160 pixels). Nominal focus 33 mm.

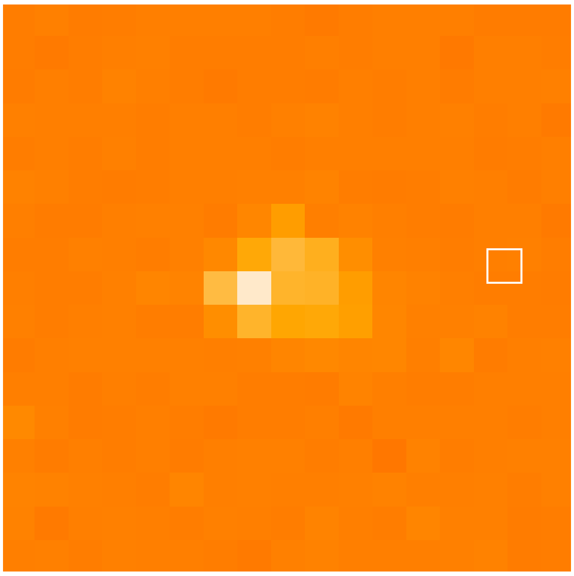

FIGURE 25. Out of focus point image at focus 28 mm (x = 226 to 242 pixels, y= 144 to 160 pixels). Nominal focus 33 mm.

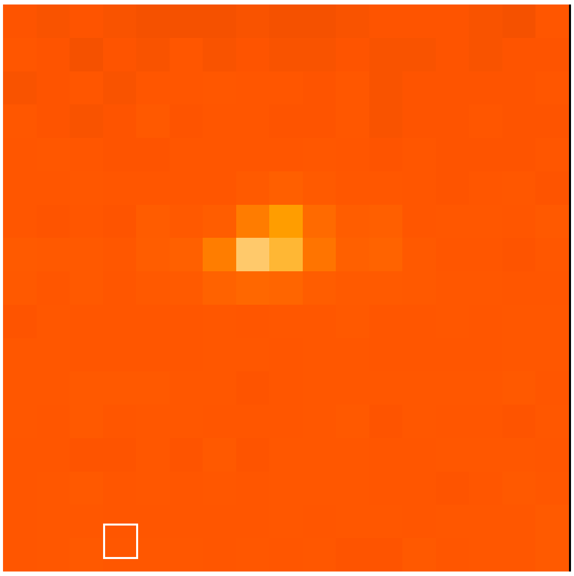

FIGURE 26. Out of focus point image at focus 28 mm (x = 49 to 65 pixels, y= 7 to 23 pixels). Nominal focus 33 mm.

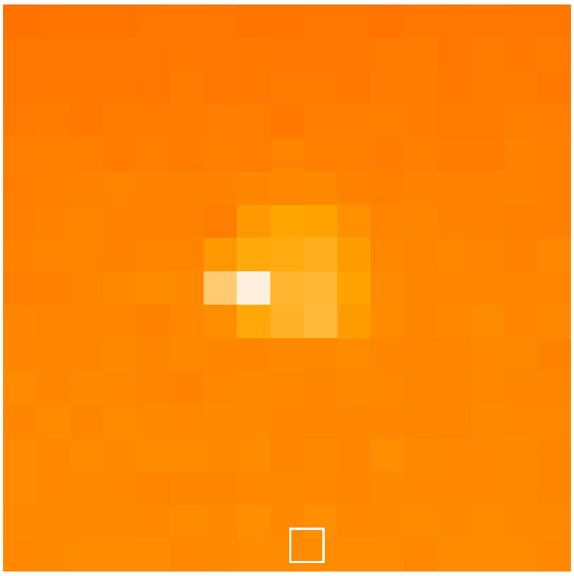

FIGURE 27. Out of focus point image at focus 28 mm (x = 138 to 154 pixels, y= 5 to 21 pixels). Nominal focus 33 mm.

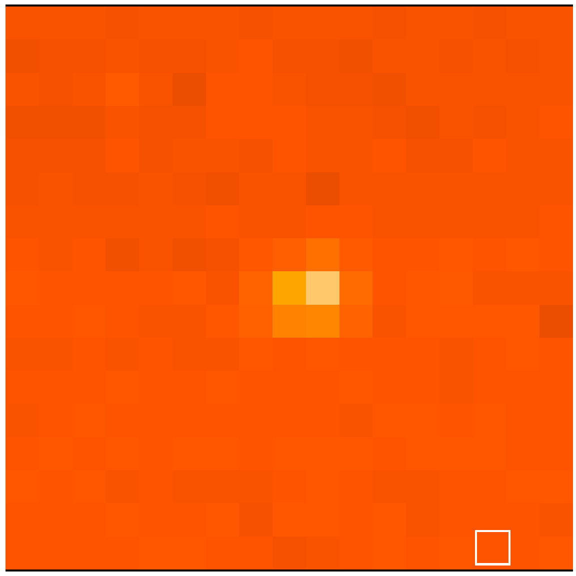

FIGURE 28. Out of focus point image at focus 28 mm (x = 226 to 242 pixels, y= 3 to 19 pixels). Nominal focus 33 mm

2.5 Conclusions

Cryogenic problem

vignetting of pupil in spectroscopy

K-band efficiency good

alignments of detector

nominal focus of dummy 1.09 mm

detector after dismounting from ISAAC 2.64

focus = 2.64 nominal 1,09

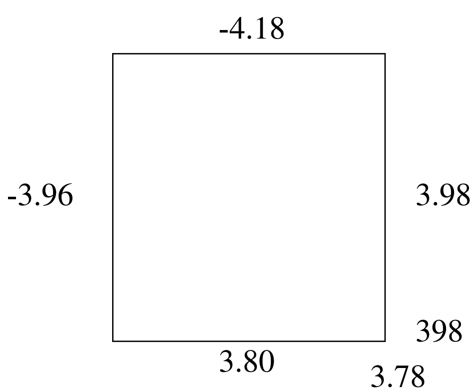

3.0 Test 3

17.3.1997

Use detector board with MOSFETS

vdet 1.084 correspond to 42 K SBRC calibration

15.4.1997

dummy detector was adjusted to 1.5 mm ----> 11.4 mm between last lens surface of L2 and detector

new value dummy detector with cryo opamps should be 1.6 mm (value from J.L. Lizon)

dummy at 1.05+/-0.01 mm   (larger value larger distance surface microscope)

InSb detector as mounted during ISAAC TEst Nr 5: at 2.60 mm

-------------> detector is 1.55 closer to the objective than dummy

angle 4.01/4.05 over array 30 micron ---------> 1 pixel/256 pixels

4.0 Test 4

5.0 Test 5

6.0 Test 6

6.1 General

For the first time both Rockwell and SBRC high doped cooled and read out with 8 channel IRACE.

6.2 Cryogenics

There is a large temperature difference of almost 20 K between coldfinger and detector temperature which is not understood. A temperature change of 1 K at the coldfinger is equivalent to a change of 12 K at the detector. The temperature change is much faster at the cold finger than at the detector.

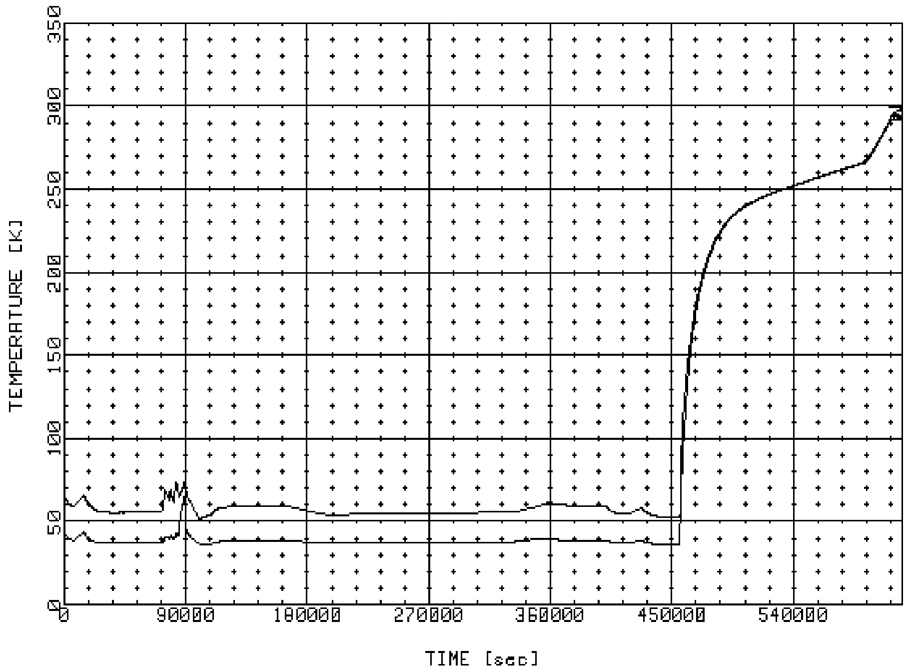

FIGURE 29. Detector temperature versus time. Lower curve: Temperature measured with on chip sensor using calibration in IRATEC. Upper curve: Temperature measured with ISAAC sensor in cold finger.

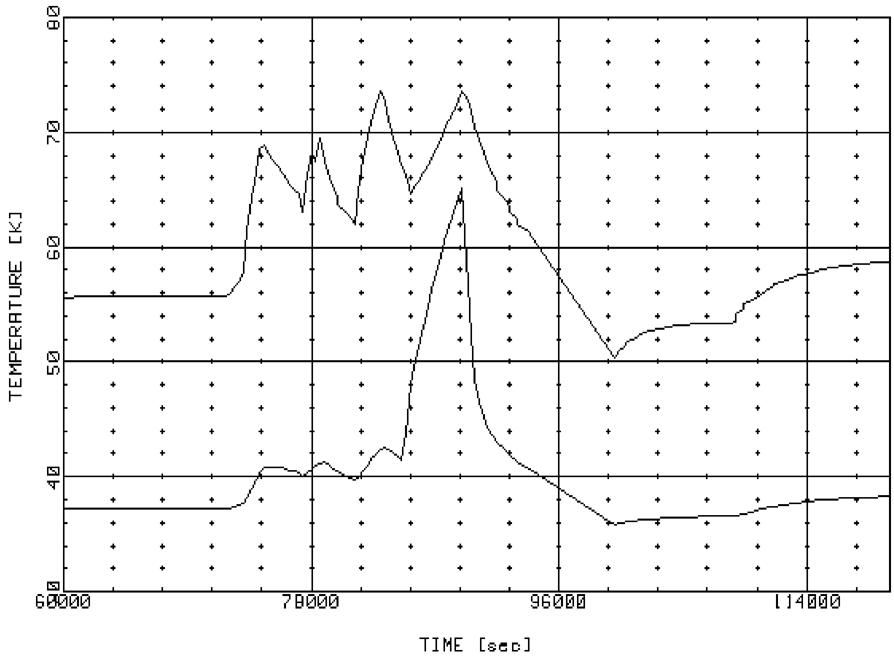

FIGURE 30. Detector temperature versus time. Lower curve: Temperature measured with on chip sensor using calibration in IRATEC. Upper curve: Temperature measured with ISAAC sensor in cold finger.

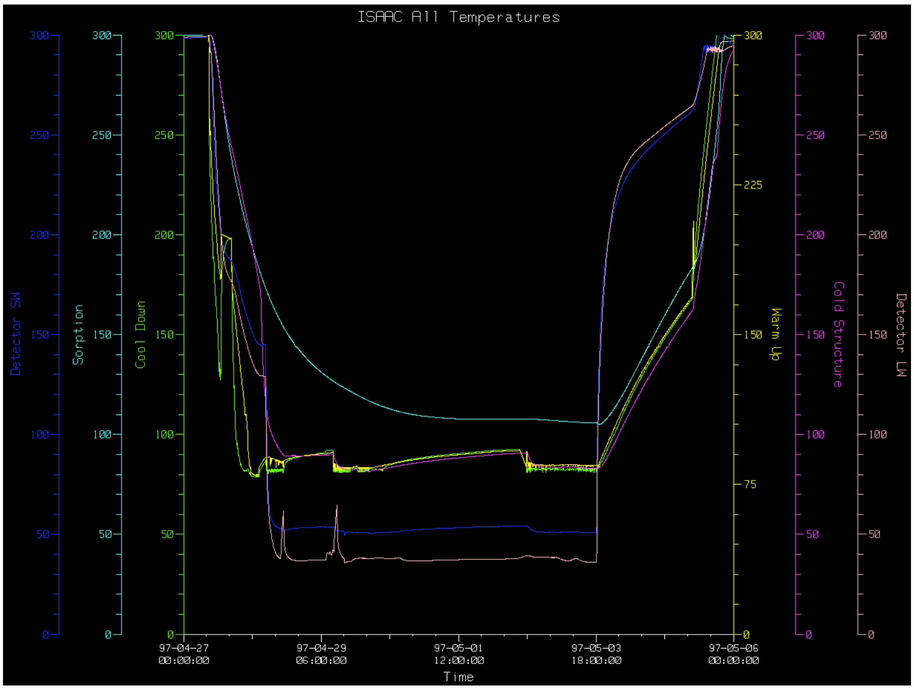

FIGURE 31. ISAAC temperatures versus time.

6.3 Darkcurrent in short wavelength channel

The PTF was measured in IRATEC using the same detector board but different supply voltages for the cryo opamps (5 V in IRATEC) and a different AQUI board.The PTF is 3.69 ADU's / electron. The darkcurrent is 204 e/hour. The first few data points are not used because of persistence effects. The temperature measured at the cold finger of the short wavelength arm was 53.54 K.

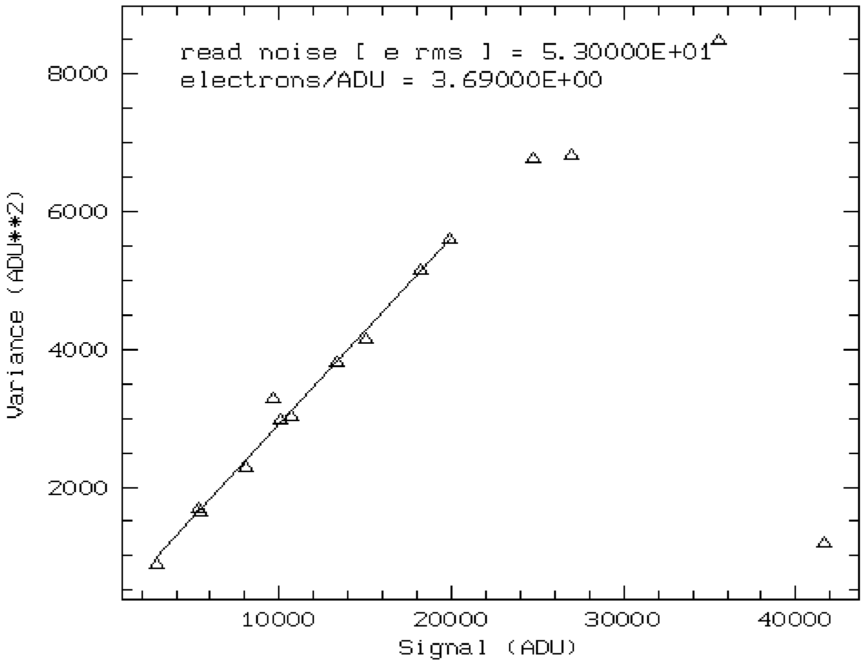

FIGURE 32. Pixel transfer function

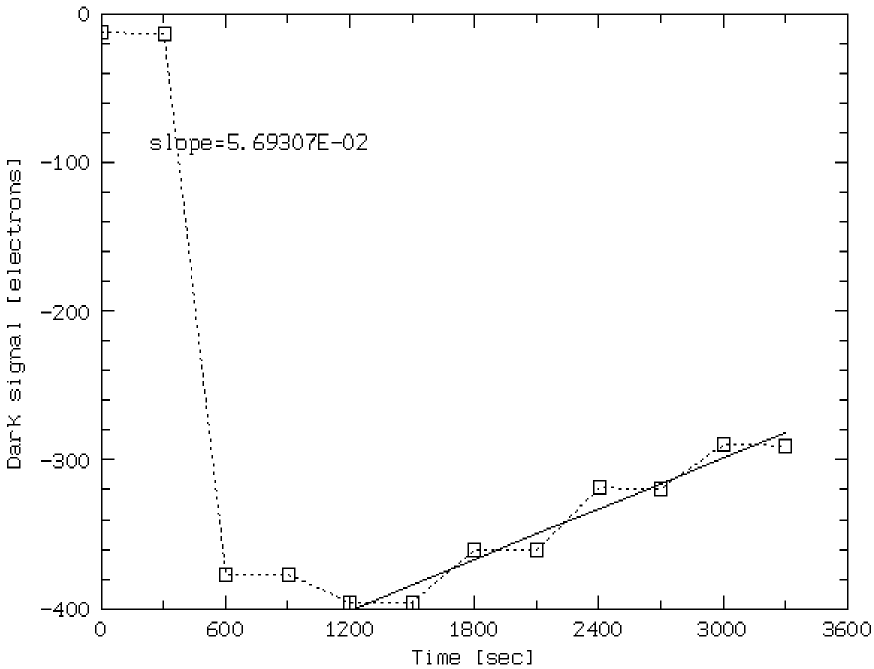

FIGURE 33. Dark signal versus time in ISAAC short wavelength channel.
Darkcurrent is 204 e/hour at

6.4 Alignment of Rockwell engineering grade 2 array

dummy at 1.05 mm (distance microscope - dummy for focus on dummy surface)

agreed position of detector: put detector 1.6 mm closer to ISAAC objective than dummy (e.g. move detector towards microscope objective), microscope position = 1.05mm + 1.6 mm = 2.65 mm,

correct for d = 130 µm saphire substrate (n = 1.73 at λ = 2.5 µm) implies correction of d/n = 190 µm, with microscope position = 1.05mm + 1.6 mm + 0.19mm = 2.84 mm focus on saphire surface.

It is not possible to go beyond 2.75 mm.

thin epoxy frame by 1 mm ---> focus to 2.84 mm

-9.44<--->-9.65 ----> 190 µm ---> 0.5 degrees tilt of array moving microscope left right

9.41<---->9.78 -------> 370 µm----> 1.12 degrees tilt moving microscope up down

According to Bernard:

S2 at 77 K in filter K broadband:

TABLE 3. Back focal distance versus collimator position for S2 and broadband K

Back focal distance [mm]	slit - collimator distance [mm]
20.39	229
20.86	219

encoder position of collimator -18000 close to slit, 22000 close to detector

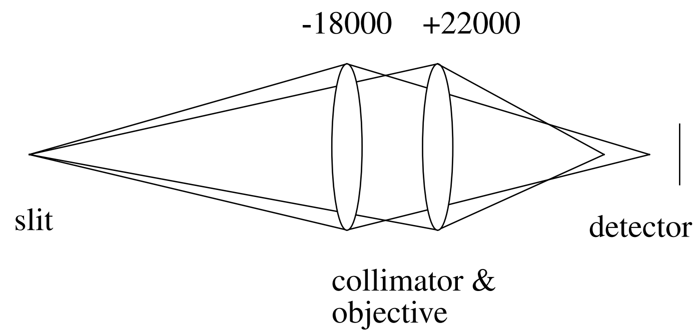

FIGURE 34. Detector position at cooldown #6. Best position of collimator -19000. Detector has to be moved closer to the objective.

According to Jean Louis BFD is 12.03 mm for L2 cooldown #5. Detector was 1.5 mm closer to objective than the dummy.

6.5 Focus determined with star simulator

For the long wavelength arm (objective L2, L3) the collimator position was at 17000 steps. For the short wavelength arm the collimator position was -13000 steps. One step corresponds to 0.234 µm. A shift of 1mm of the star simulator focus corresponds to 10000 encoder steps. In the curves below the focus position in mm was calculated as:

$$Position = 14.8 - \frac{(encodersteps)}{10000}$$

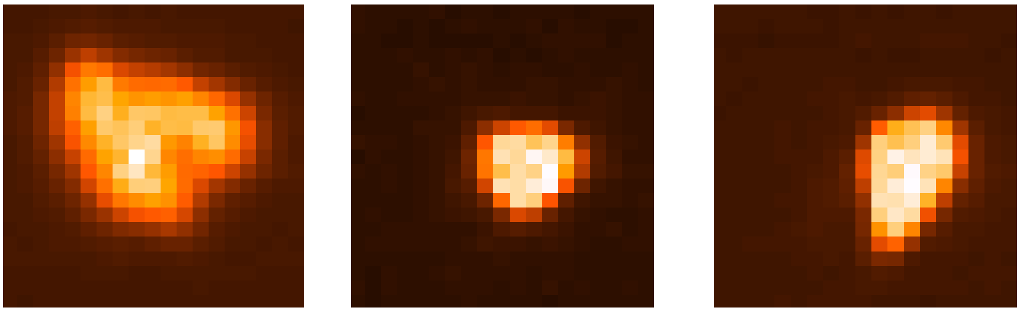

FIGURE 35. Image quality of L3 measured with star simulator in broadband K for different positions of star simulator focus. Left: -1.2 mm (160000 steps). Middle: -8.2 mm (230000 steps). Right: -13.2 mm (280000 steps)

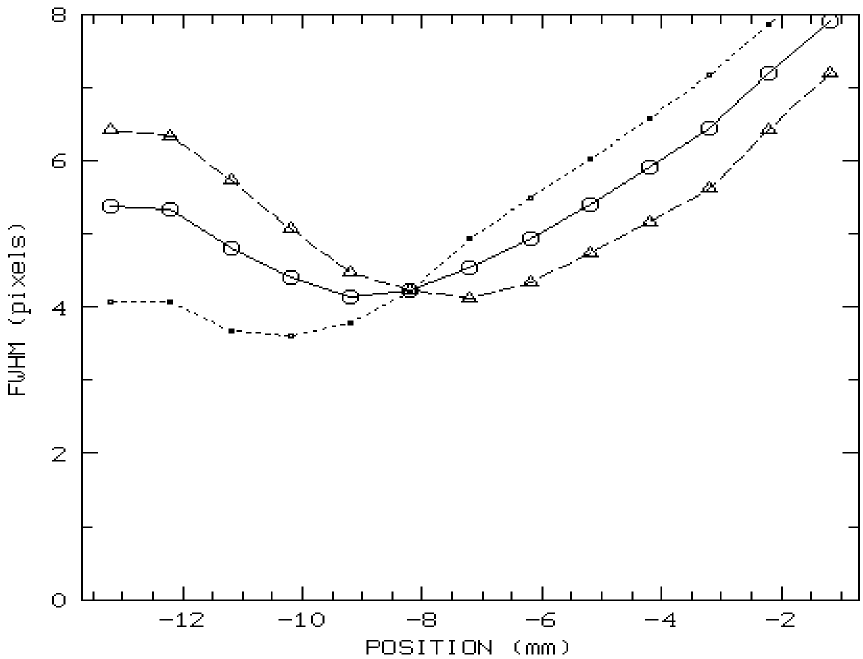

FIGURE 36. Focus curve for objective L3 in broadband K. Circles: averaged FWHM. Dots: FWHM in x direction. Triangles: FWHM in y direction. Position with respect to slit. Positive direction pointing from slit towards collimator. Focus of star simulator in zero position is assumed to be 14.8 mm in positive direction wrt slit.

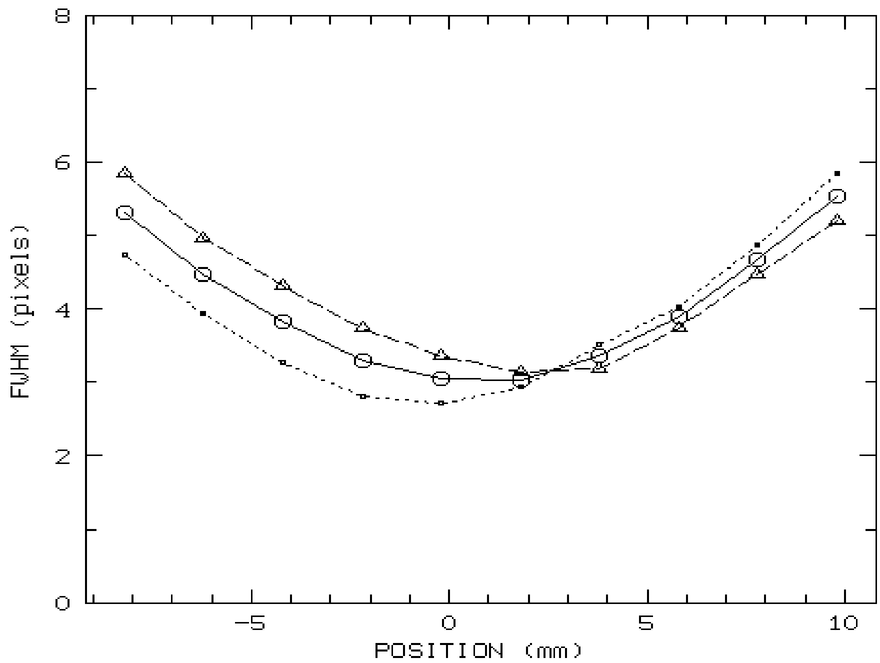

FIGURE 37. Focus curve for objective L2 in broadband K. Circles: averaged FWHM. Dots: FWHM in x direction. Triangles: FWHM in y direction. Position with respect to slit. Positive direction pointing from slit towards collimator. Focus of star simulator in zero position is assumed to be 14.8 mm in positive direction wrt slit. Encoder position 17000

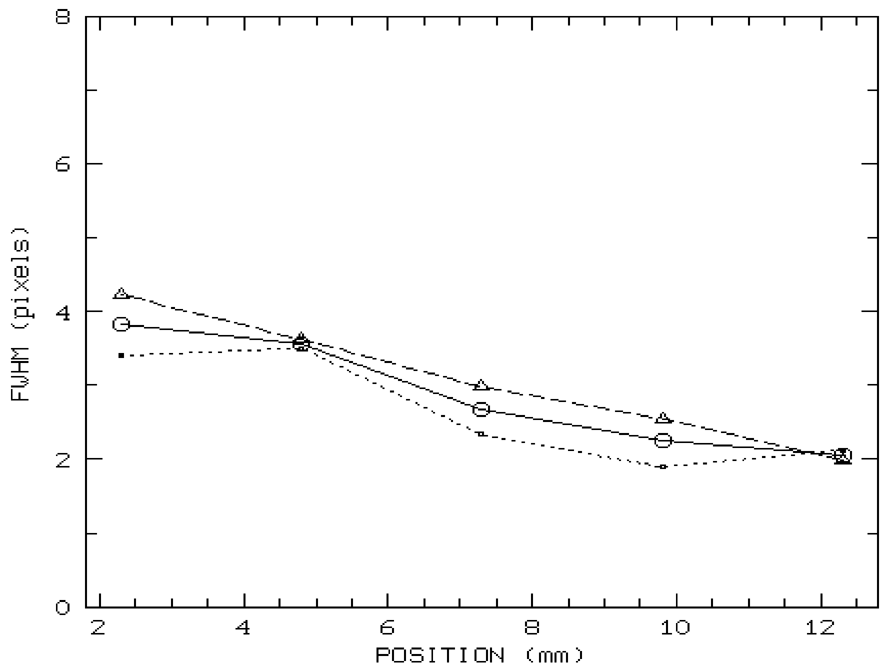

FIGURE 38. Focus curve for objective S2 in broadband K. Circles: averaged FWHM. Dots: FWHM in x direction. Triangles: FWHM in y direction. Position with respect to slit. Positive direction pointing from slit towards collimator. Focus of star simulator in zero position is assumed to be 14.8 mm in positive direction wrt slit.

The focus curve measured with S2 by scanning the star simulator is in conflict with the focus curves measured by scanning the collimator lens.

6.6 Conclusion

Due to an alignment error of 1 mm the distance between detector and the last optical surface of the objective has to be reduced by 1 mm.

agreed position of detector: put detector 2.6 mm closer to ISAAC objective than dummy (e.g. move detector towards microscope objective),

7.0 Test 7

SBRC256: microscope position = 1.05mm + 2.6 mm = 3.65 mm

Hawaii eng2 microscope position = 1.05mm + 1.6 mm + 0.19mm +0.5 = 3.34 mm (set to 3.30mm. 500 micron tilt

SBRC mount spacer in soccket 1mm+0.57mm = 1.57mm

clock 2 -.2/+.2 for cryo opamp

Saturation in K broad and narrow band (2.28)

7.1 Saturation

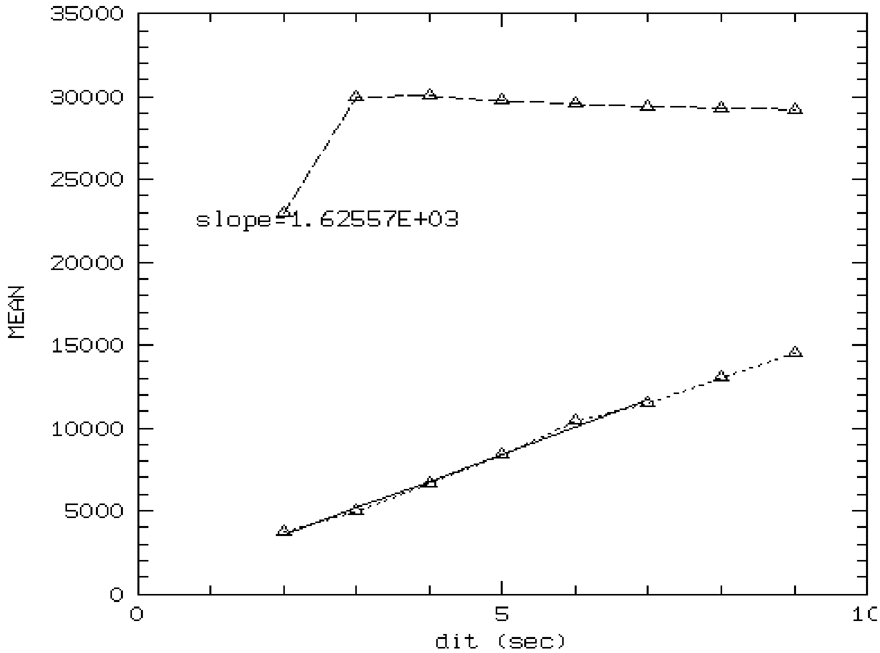

FIGURE 39. Room temperature seen with S2 in brad and narrow band K. For broadband K and dit= 2 sec Signal is 22881ADU.

satu_sw_ima_open_K, satu_sw_ima_open_NB_2_28

7.2 Darkcurrent

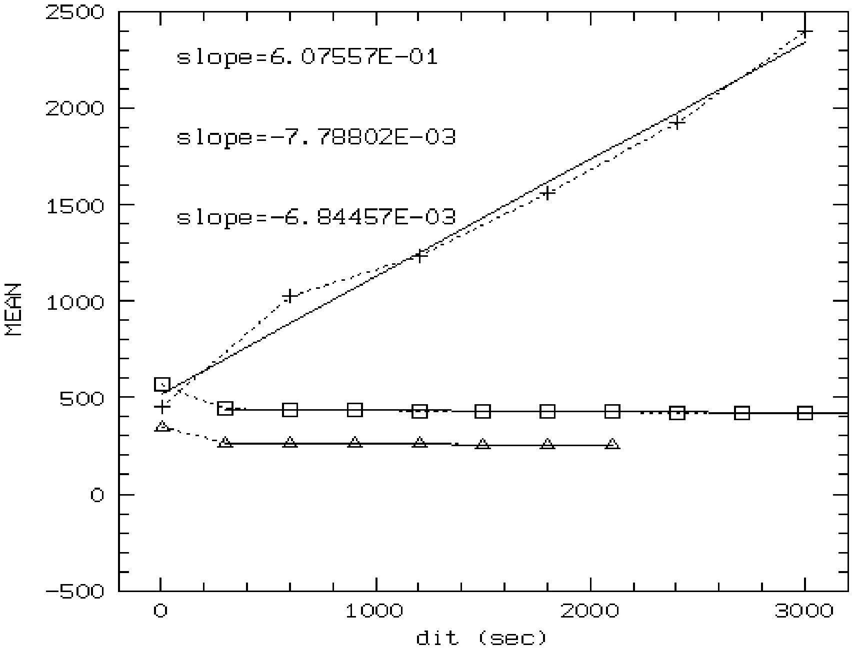

FIGURE 40. Dark versus time. Square: slitmask wheel and filter wheel both closed (-103 e/h). Cross: slitmask wheel open, filter wheel closed (8070e/h). Triangle: slitmaskwheel slit filter closed (-90e/h).

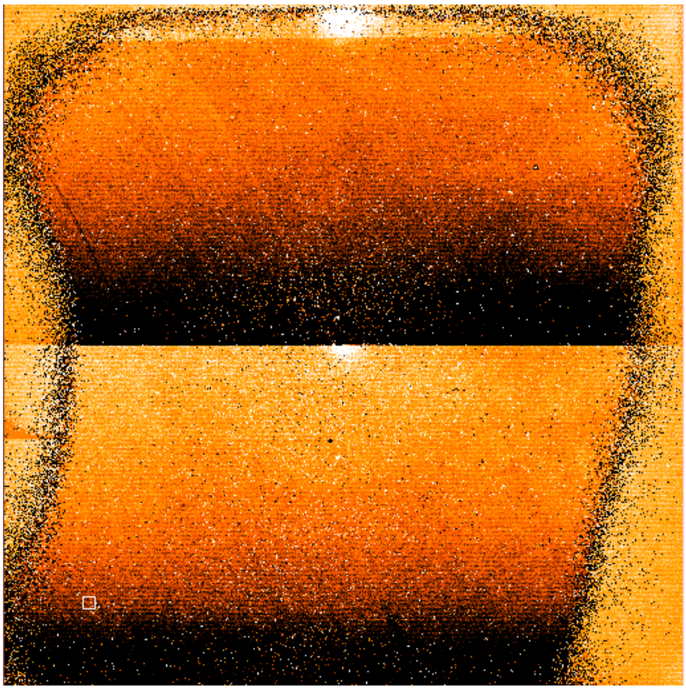

FIGURE 41. 1800 sec exposure (2102-302 sec) with slit and filter dark. Cuts -25/+25 ADU.

7.3 Focus of star simulator

Lens L2

TABLE 4.

cooldown	detector position	collimator position	best focus
6	0 mm	17000	+1.5 mm
7	1 mm	5000	-19mm

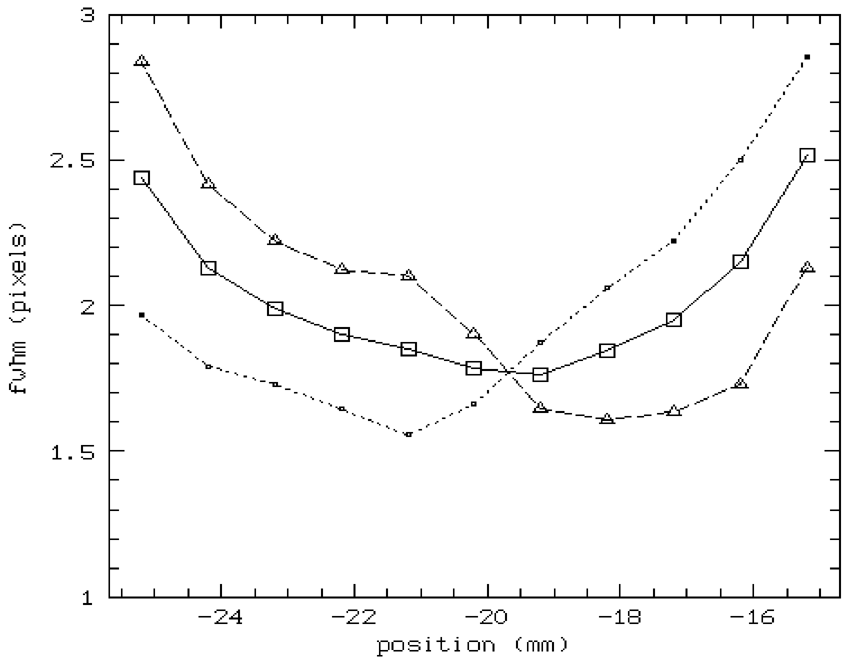

FIGURE 42. Focus curve for objective L2 in broadband K. Circles: averaged FWHM. Dots: FWHM in x direction. Triangles: FWHM in y direction. Position with respect to slit. Positive direction pointing from slit towards collimator. Focus of star simulator in zero position is assumed to be 14.8 mm in positive direction wrt slit. Encoder Position of collimator 5000.

7.4 Image Quality S2

measured with star simulatoron axis:

247.376

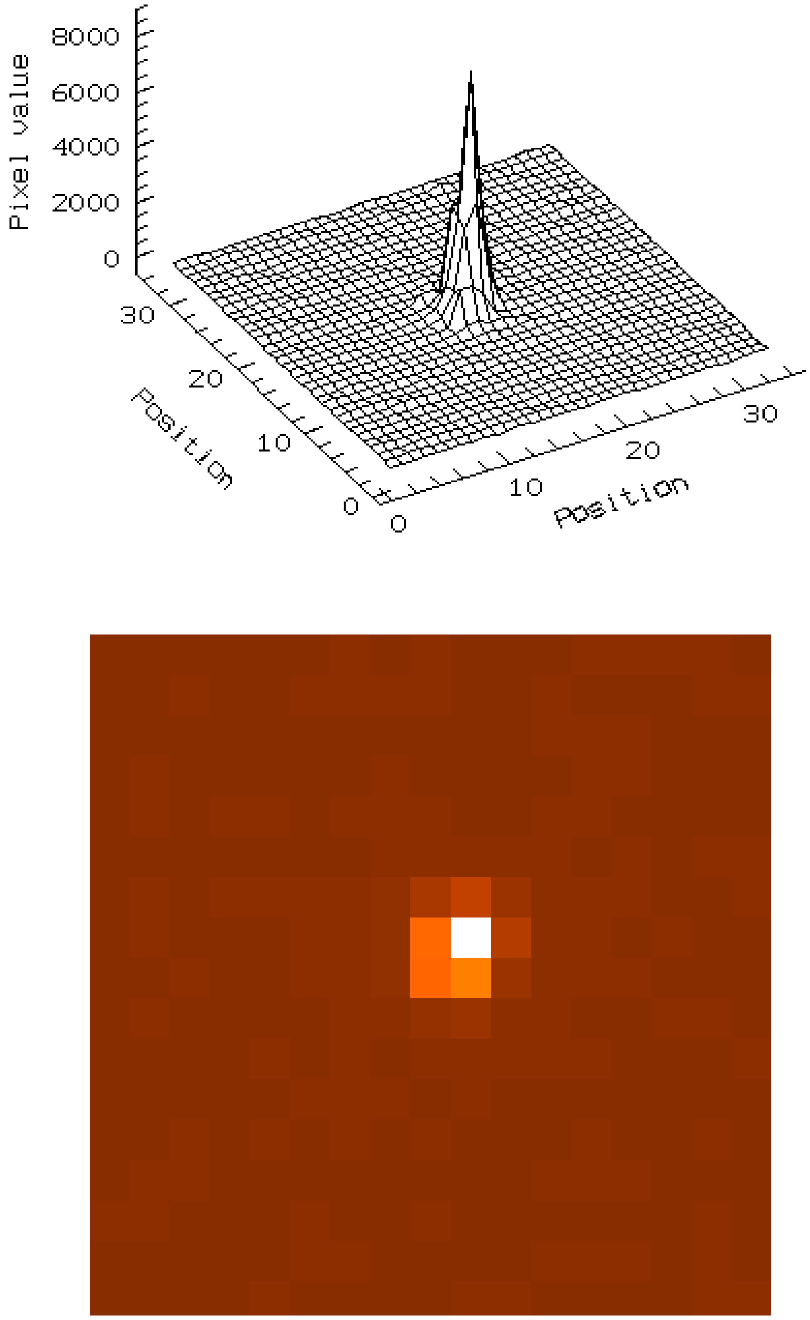

FIGURE 43. Image quality of S2 in Brγ 0.43% of total flux on 1 pixel. Fwhm 1.15 pixels. Center pixel 2591 ADU.

magnification measured 0.216 , nominal 0.217 (F/3.26 assumed for S2)

7.5 Efficiency

The overall efficiency of the instrument was determined by varying the temperature of a blackbody which is imaged to the telescope focus by the star simulator. The variance of the signal is plotted versus the signal. The inverse slope yields the pixel transfer function in electrons per ADU assuming that the increase of noise is due to the increase of flux and associated shot noise. One ADU corresponds to 2.85+/-0.06 electrons as shown in Figure 44.

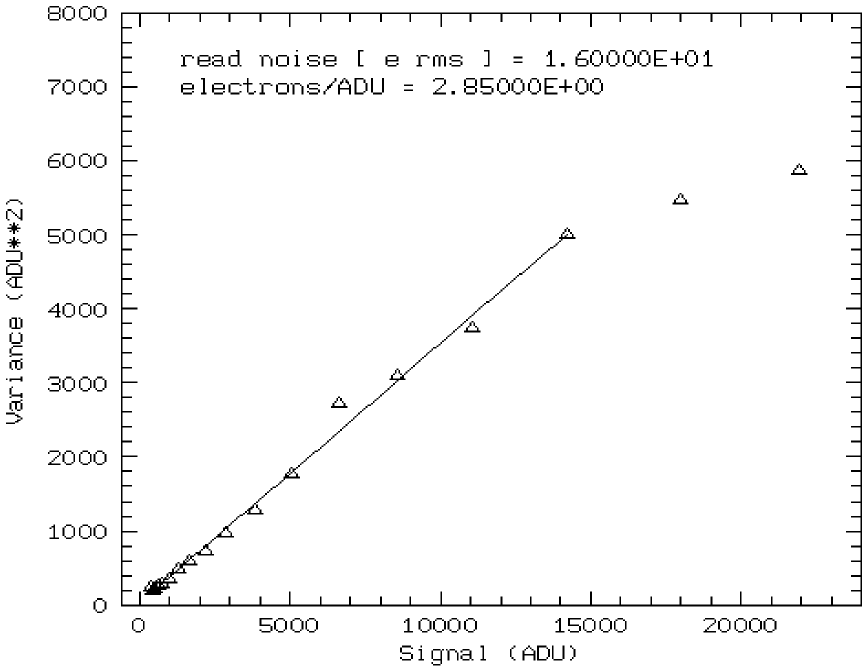

FIGURE 44. Pixel transfer function determined with shot noise method.

The objective S2 was used in the imaging mode with both the broadband filter K' and the narrow band filter Brγ in the optical beam at the same time . The blackbody temperature was varied between 10 and 100 C in steps of 5 degrees. The photon flux was calculated taking into account the bandpass of the Brγ filter and assuming the focal ratio of S2 being f/3.24. The PTF measurement allows to plot the number of detected electrons versus the number of calculated photons yielding an overall efficiency of the instrument including the star simulator the K' filter and the QE of the detector. The value obtained from Figure 46 is 0.341+/-0.001. The reflection loss of the two CaF_2 lenses in the star simulator is 0.88 an the QE of the detector measured in IRATEC was 0.66. The resulting overall optical efficiency of ISAAC in the imaging mode at λ=2.166 µm with objective S2 is 0.59. For comparison, the expected optical efficiency is 0.71. Including the QE of the detector the overall efficiency of ISAAC is 0.39.

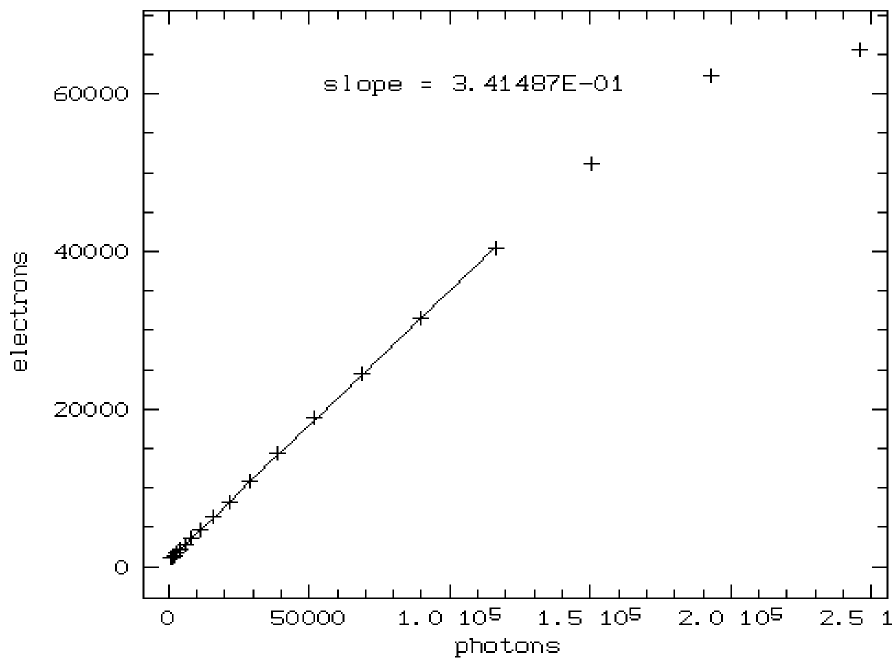

FIGURE 45. Efficiency of ISAAC in imaging mode using S2 at Brγ including efficiency of star simulator and quantum efficiency of detector is 0.34. Optical efficiency is 0.59. Overall efficiency including detector is 0.39. Saturation level of detector is 6 10^5.

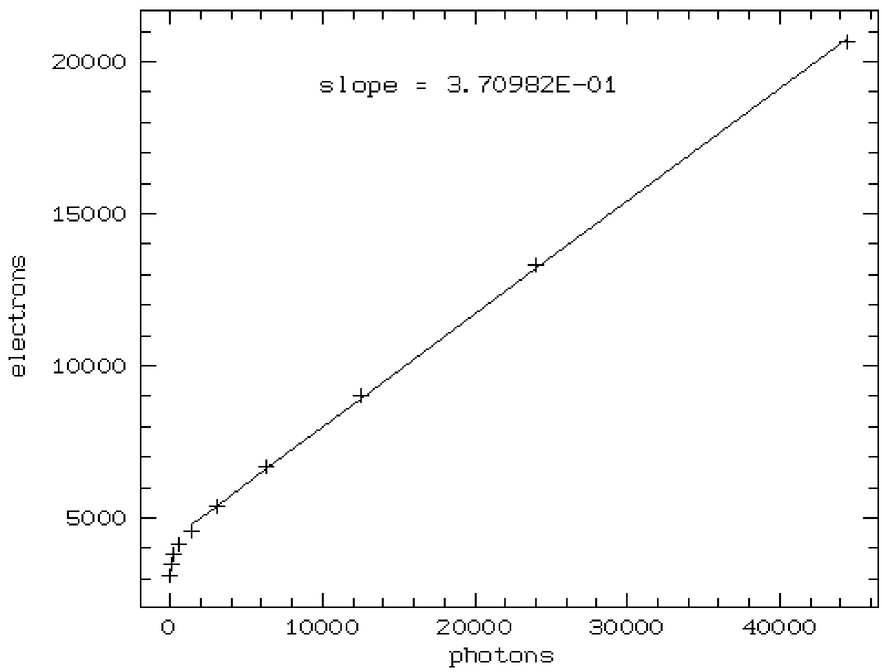

FIGURE 46. Efficiency of ISAAC in imaging mode using S2 and broadband H filter including efficiency of star simulator and quantum efficiency of detector is 0.37. Optical efficiency is . Overall efficiency including detector is .

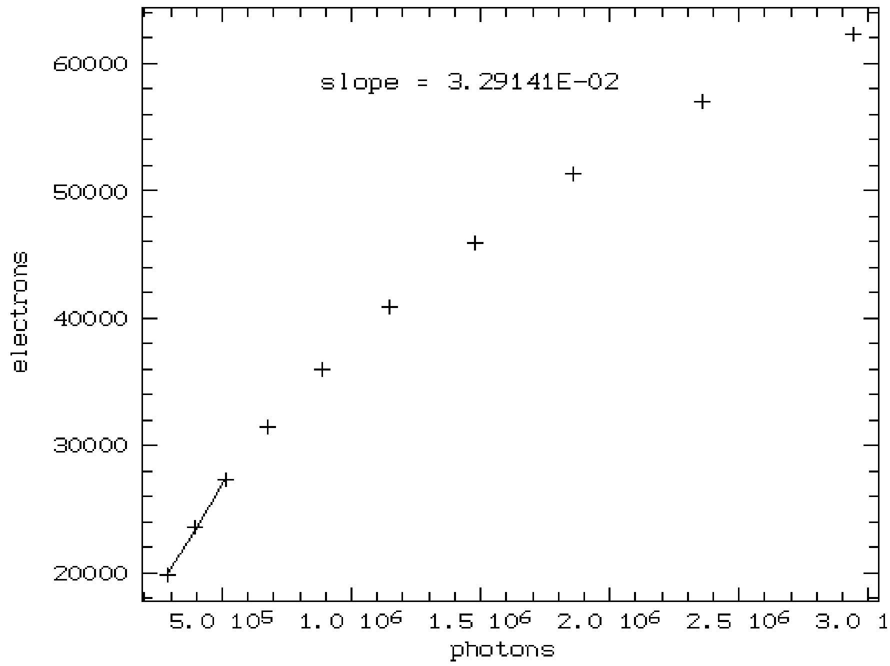

FIGURE 47. Efficiency of ISAAC in imaging mode using S2 and broadband narrow band filter 1.125 µm filter including efficiency of star simulator and quantum efficiency of detector is 0.033. Optical efficiency is . Overall efficiency including detector is .

7.6 Image quality of S2 measured by spot scan.

The output of a single mode IR fiber having a diameter of 6.5 µm was re-imaged by the star simulator to the telescope focus. The star simulator which is mounted on a xyz translator stage was stepped in a grid of 10 µm. The input of the fiber was illuminated by a blackbody at a temperature of 140 Celsius. Using the spectral filter Brγ at λ=2.121 µm images were taken as difference with the shutter in front of the blackbody in the open and closed position. The ISAAC objective has a focal ratio of f/3.26 and a demagnifies the image of the telescope focus on the detector by a factor of of .216. The radius of the airy disk at the used wavelength was 8.46 µm.

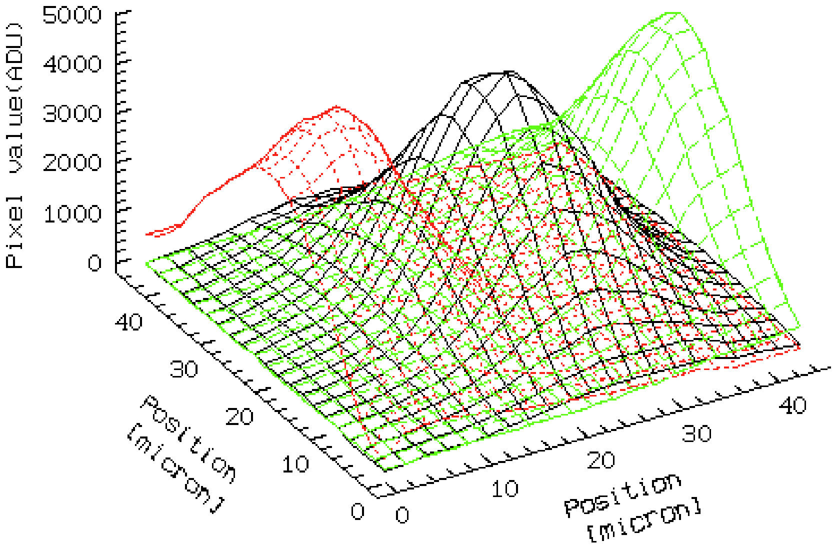

FIGURE 48. Spot scan of Hawaii 1024x1024 MCT array in steps of 2.16 µm x 2.16 µm.